Binary-encounter form factor and its use in the calculation of inelastic cross sections involving Rydberg atoms

F. Gounand and L. Petitjean
Service de Physique des Atomes et des Surfaces, Institut de Recherche Fondamentale, Commissariat à l'Energie Atomique, Centre d'Etudes Nucleaires de Saclay, F-91191 Gif-sur-Yvette Cedex, France
(Received 1 December 1983)

The form factor is a key parameter to be evaluated in most theoretical approaches currently available for the calculation of inelastic collisional cross sections involving Rydberg atoms. The binary-encounter method is shown to offer a very powerful means for the rapid evaluation of this parameter. Analytical expressions of the form factor are derived from hydrogenic wave functions. Many comparisons between binary-encounter and quantal calculations establish the range of validity of the former method. It is shown that, in most situations of practical interest, this approach provides an easy and efficient way to compute the cross sections corresponding to inelastic collisions between Rydberg atoms and atomic or molecular targets.

I. INTRODUCTION

Collisions between Rydberg atoms and atomic (or molecular) targets have been the subject of numerous theoretical and experimental investigations in the recent past.[1] Various theoretical approaches have been developed and extensive comparisons between theory and experiment allow some general conclusions to be drawn concerning the interaction responsible for such processes. In many cases it is now recognized that the interaction between the outer slow electron and the neutral target is responsible for the depopulation of Rydberg atoms. If this interaction only is taken into account the n and l dependences of the cross section can be reproduced reasonably well. Moreover quantitative agreement between observed and calculated cross sections has been obtained in most cases. These calculations predict that Rydberg atoms are mainly depopulated towards hydrogenic levels of high multiplicity, a theory supported by experimental observations. More precisely, for Rydberg-atom—ground-state-atom collisions it is the closest hydrogenic manifold which represents the main exit channel, no potential energy change occurring for the ground-state atom. In the case of molecular targets the situation is different because of the internal degrees of freedom of the molecule (in fact, rotation alone is involved at thermal energies) and hydrogenic manifolds with significant energy changes can be reached. Under these conditions the molecular target undergoes an inelastic process also. This situation can occur, in fact, as long as the target possesses bound (or continuum) states which are energetically accessible in the collision process; as, for example, in the case of excited atomic targets.

Among the various approaches accounting only for the $(e^-\text{-}\mathscr{P})$ interaction ($\mathscr{P}$ perturber), those derived from the impulse approximation[2] have proved very efficient for the cross-section calculations.[3,4] According to the impulse approach (the validity of which has been widely investigated[5–7] and will not be discussed here) the cross section σ_{if} for the $(i \to f)$ transition takes the form

$$\sigma_{if} = \frac{2\pi}{v^2} \int_{K_{\min}}^{K_{\max}} |f_e(K)|^2 F_{if}(K) K \, dK \tag{1}$$

(atomic units are used throughout the paper, unless specified), where v is the relative velocity of the colliding partners, $f_e(K)$ is the $(e^-\text{-}\mathscr{P})$ scattering amplitude for a given momentum transfer K, and $F_{if}(K)$ is the squared form factor for the given transition, i.e.,

$$F_{if}(K) = |\langle f | e^{i\vec{K}\cdot\vec{r}} | i \rangle|^2 , \tag{2}$$

$\vec{r}$ being the coordinate of the Rydberg electron. The integration range in Eq. (1) is determined from energy conservation consideration. Usually a very simple form for $f_e(K)$ can be assumed, dependent on the nature of the $(e^-\text{-}\mathscr{P})$ interaction (e^--atom, e^--dipole, e^--quadrupole, ...). Thus, form-factor evaluation is a key step in the derivation of the cross section.

Many publications have been devoted to an evaluation of the form factor.[8–11] For our purpose it is sufficient to sum up the situation as follows: If hydrogenic wave functions are used, the quantal expression of the squared form factor for a $n,l \to n',l'$ transition can be derived in analytical form, but the corresponding computations are very time consuming. Moreover numerical catastrophic cancellations preclude the use of the method for n values over about 35, even when double-precision algebra is used. For higher n values it is necessary to rely on extrapolation procedures, the validity of which is difficult to assess [the situation is even worse if more sophisticated wave functions are used,[12] but for Rydberg states hydrogenic wave functions seem to provide sufficient accuracy, though in some cases numerical interpolations appear useful for nonhydrogenic initial (n,l) states[13]]. The final states to be considered being usually a hydrogenic manifold n' it is necessary to sum the corresponding $\sigma_{nl\to n'l'}$ values over l' in order to obtain a cross section comparable to a measured quenching cross section. Quantal calculations have been performed in this way for Rydberg-atom—ground-state-atom collisions up to $n \sim 35$. The case of Rydberg-

atom—molecule collisions is still more complicated since numerous n' manifolds can contribute significantly to the quenching cross section[14] (even ionization has to be considered). Semiclassical methods, mainly based on the correspondence principle,[8] have also been used to overcome the difficulty for obtaining a rapid evaluation of the form factor but the approach seems to be limited.[4] One last interesting possibility appears to be the derivation of the form factor from the binary-encounter theory (BET).[15] This method has already proved useful for bound-free transitions[9,16] (i.e., for example, Rydberg-atom—molecule collisions leading to ionization) and was also used recently by Matsuzawa for calculations of bound-bound transitions with large $|n-n'|$ values, induced by molecular targets.[17] The method is attractive because it yields the squared form factor directly for a $n,l\rightarrow n'$ transition, where n' is a hydrogenic manifold. The resulting lack of information on $n,l\rightarrow n',l'$ processes is not important since most measurements only provide total depopulation cross sections.

The main aim of this paper is to demonstrate that the use of the binary-encounter form factor (hereafter referred to as the BET form factor) enables the cross sections of a wide class of collisional processes between Rydberg atoms and neutral targets to be computed easily and efficiently, a fact not yet recognized in the literature [i.e., the BET form factor will be shown in most cases to give a good approximation of the quantal form factor over the integration range of interest in Eq. (1)]. To this end the paper is presented as follows. Section II focuses on a derivation of the BET form factor for bound-bound transitions, with emphasis on the necessary assumptions. Section III gives explicit expressions of the BET form factor. Section IV discusses the cross-section calculations for some collisional processes involving Rydberg atoms. Finally, Sec. V is devoted to the comparison between quantal and BET calculations for various situations of practical interest.

II. SQUARED BET FORM FACTOR FOR BOUND-BOUND TRANSITIONS

It is useful here to give the explicit derivation of the BET form factor in the case of bound-bound transitions since the literature seems to contain little information on the subject, unlike that of the bound-free case. The main lines of the derivation follow more or less closely the work of Vriens,[18] which draws heavily on a mathematical method first developed by Nijboer and Rahman[19] for the slow neutron scattering theory. Finally, our derivation neglects any correlation effects,[18] holding strictly for alkali-metal atoms, in order to avoid complications which are most probably unnecessary for any atomic Rydberg states.

We wish to calculate the following squared form factor:

$$F_{nl,n'}(K)=\frac{1}{2l+1}\sum_{m}\sum_{l',m'}|\langle n',l',m'|e^{i\vec{K}\cdot\vec{r}}|n,l,m\rangle|^2 \tag{3}$$

with summation over the magnetic substates of the initial state $|n,l,m\rangle\equiv|i\rangle$. The final state n' is first assumed to be hydrogenic, i.e., all $|n',l',m'\rangle\equiv|f\rangle$ substates have the same energy $E_f=-1/2n'^2$. Let us for convenience rewrite Eq. (3) as

$$F_{nl,n'}(K)=\frac{1}{2l+1}\sum_{m}\sum_{f}|\langle f|e^{i\vec{K}\cdot\vec{r}}|i\rangle|^2, \tag{4}$$

where the summation over f covers all final states $|n',l',m'\rangle\equiv|f\rangle$ of energy E_f. For high enough n' values we write

$$F_{nl,n'}(K)\simeq\frac{1}{2l+1}\sum_{m}\sum_{f}\frac{1}{n'^3}\delta(E_f-E_i-E)\times|\langle f|e^{i\vec{K}\cdot\vec{r}}|i\rangle|^2, \tag{5}$$

where E_i is the energy of the initial (n,l) state. Here the summation over f covers the whole energy spectrum (bound and continuum states). Equation (5) holds only for sufficiently high n' values since the n'^{-3} factor accounts for the density of final states per unit energy, the δ function ensuring the selection of those hydrogenic bound states with energy E_f. Note that this procedure is equivalent to that used to obtain the continuity relation for the density of generalized oscillator strengths at the ionization limit.[10] We now express the δ function by its Fourier transform, i.e.,

$$\delta(E_f-E_i-E)=\frac{1}{2\pi}\int_{-\infty}^{+\infty}e^{i(E_f-E_i-E)t}dt, \tag{6}$$

where the integration variable may be interpreted as time. Using this expression, the closure relation for the final states $|f\rangle$, and the relations

$$e^{iE_it}|i\rangle=e^{iHt}|i\rangle\ (\mathrm{TV}), \tag{7}$$

$$e^{i\vec{K}\cdot\vec{r}(t)}=e^{iHt}e^{i\vec{K}\cdot\vec{r}}e^{-iHt}\ (\mathrm{HR}), \tag{8}$$

(where TV is the time variation and HR is the Heisenberg representation) we finally obtain

$$F_{nl,n'}(K)\simeq\frac{1}{(2l+1)n'^3}\times\sum_{m}\frac{1}{2\pi}\int_{-\infty}^{+\infty}e^{-iEt}\langle i|e^{-i\vec{K}\cdot\vec{r}(0)}\times e^{i\vec{K}\cdot\vec{r}(t)}|i\rangle dt. \tag{9}$$

The second necessary assumption (the first being that n' is high enough) is that the excited electron in state $|i\rangle$ is free during the collision, i.e.,

$$\vec{r}(t)\simeq\vec{r}(0)+\vec{v}t \tag{10}$$

to first order in time [note that Eq. (10) holds to all orders for a free Hamiltonian]. Thus the approximation corresponds to ignore the effect of the binding (Coulomb) potential during the collision and consequently requires n to be sufficiently large. It is clear from Eq. (8) that the use of this first-order approximation [Eq. (10)] limits the validity of the derivation to small enough K values. For high-K values, higher-order terms should be included in Eq. (10) if the diagonal matrix element of Eq. (7) is to be

calculated accurately. Using Eq. (4) and the Weyl's operator identity, i.e.,

$$e^{A+B}\equiv e^{A}e^{B}e^{-\frac{1}{2}[A,B]} \tag{11}$$

which holds, provided that the commutator $[A,B]$ commutes both with A and with B, we obtain

$$F_{nl,n'}(K)\simeq\frac{1}{(2l+1)n'^{3}}\sum_{m}\langle i\,|\,\delta(\vec{\mathrm{K}}\cdot\vec{\mathrm{v}}+\tfrac{1}{2}K^{2}-E)\,|\,i\rangle\ , \tag{12}$$

where $\vec{\mathrm{v}}$ is the only variable. Note, as already pointed out,[9] the similarity between Eq. (12) and the Compton profile[20] (bound-free transition) obtained with the impulse approximation. The final integration can now be performed in the momentum (velocity) space, leading to:

$$F_{nl,n'}(K)\simeq\frac{1}{(2l+1)n'^{3}}\sum_{m}\int_{0}^{\infty}dp\,p^{2}\int_{\Omega}|\,g_{nl}(p)\,|^{2}Y_{lm}^{*}(\Omega)Y_{lm}(\Omega)\delta(\vec{\mathrm{K}}\vec{\mathrm{v}}+\tfrac{1}{2}K^{2}-E)d\Omega\ , \tag{13}$$

where $g_{nl}(p)$ is the momentum wave function and $Y_{lm}(\Omega)$ represents the usual spherical harmonics. Finally, using the summation of spherical harmonics and choosing the polar axis along the momentum transfer $\vec{\mathrm{K}}$ (i.e., writing $\vec{\mathrm{K}}\cdot\vec{\mathrm{v}}=K\vec{\mathrm{v}}\cos\theta$, with $-1<\cos\theta<1$), we obtain

$$F_{nl,n'}(K)\simeq\frac{I(p_0)}{2n'^{3}K}=\frac{1}{2n'^{3}K}\int_{|p_0|}^{\infty}|\,g_{nl}(p)\,|^{2}p\,dp \tag{14}$$

with

$$p_0=\frac{E_f-E_i-\frac{1}{2}K^{2}}{K}\ . \tag{15}$$

Equations (14) and (15) are the basic equations for the bound-bound BET form factor which will be used extensively in the following sections. The necessary assumptions can be summarized as follows: n and n' large and K small. Precise validity criteria for Eq. (14) are difficult to define; this point will call for a separate study and we shall therefore rely on the comparison between BET and quantal calculations to check the accuracy of Eq. (14).

III. BET SQUARED FORM FACTOR USING HYDROGENIC WAVE FUNCTIONS

The problem reduces to the evaluation of $I(p_0)$ [see Eq. (14)]. We start from the well-known expression of the $g_{nl}(p)$ function,[21] namely,

$$g_{nl}(p)=2^{2l+2}n^{2}l!\left[\frac{2}{\pi}\frac{(n-l-1)!}{(n+l)!}\right]^{1/2}\frac{(np)^{l}}{(n^{2}p^{2}+1)^{l+2}}\times C_{n-l-1}^{l+1}\left[\frac{n^{2}p^{2}-1}{n^{2}p^{2}+1}\right], \tag{16}$$

where C_{n-l-1}^{l+1} is a Gegenbauer polynomial,[22] which may be expressed in terms of hypergeometric functions. However, the corresponding expression leads to numerical problems at high-n values when the integral in Eq. (15) is evaluated. This difficulty can be overcome as follows: taking

$$\cos x=(n^{2}p^{2}-1)/(n^{2}p^{2}+1)$$

and changing the range of integration accordingly we finally get

$$I(p_0)=I(x_0)=\frac{2^{2l+3}n^{2}(l!)^{2}}{\pi}\frac{(n-l-1)!}{(n+l)!}\times\int_{0}^{x_0}\sin^{2l+1}x\,\sin^{4}(\tfrac{1}{2}x)\times|\,C_{n-l-1}^{l+1}(\cos x)\,|^{2}dx \tag{17}$$

with

$$x_0=\arccos[(n^{2}p_0^{2}-1)/(n^{2}p_0^{2}+1)]\ ,$$

p_0 being determined by Eq. (15).

We now develop the procedure by which Eq. (17) can be reduced to a finite series. First we expand the Gegenbauer polynomial in terms of trigonometric lines,[23] i.e.,

$$C_{n-l-1}^{l+1}(\cos x)=\frac{1}{(l!)^{2}}\sum_{i=1}^{N-1}a_i\cos[(N-2i)x] \tag{18}$$

with $N=n-l+1$ and

$$a_i=\frac{(i+l-1)!(n-i)!}{(i-1)!(n-i-l)!}\ .$$

The symmetry property $a_i=a_{N-i}$ allows us to write

$$|\,C_{n-l-1}^{l+1}(\cos x)\,|^{2}=\frac{1}{(l!)^{2}}\left[\sum_{\alpha=2}^{2i_{\max}}s(\alpha)\cos[2(N-\alpha)x]+\sum_{\beta=1}^{i_{\max}}d(\beta)\cos[2(\beta-1)x]\right], \tag{19}$$

where $i_{\max}$ depends on n,l, and the parity of N. The $s(\alpha)$ and $d(\beta)$ coefficients are easily derived from the a_i coefficients. Thus the evaluation of $I(x_0)$ reduces to that of the following integral:

$$\int_{0}^{x_0}\sin^{2l+1}x\,\sin^{4}(\tfrac{1}{2}x)\cos(2\gamma x)dx\ ,$$

where γ stands for $N-\alpha$ or $\beta-1$. It can be shown that

$$\sin^{2l+1}x \sin^4(\tfrac{1}{2}x)=\sum_{j=1}^{2l+3} C_l(j)\sin(jx) , \tag{20}$$

where the $C_l(j)$ coefficients are obtained from the recursion equation

$$C_{l+1}(j)=\tfrac{1}{2}C_l(j)-\tfrac{1}{4}C_l(j-2)-\tfrac{1}{4}C_l(j+2) \tag{21}$$

starting from $C_0(1)=\frac{5}{16}$, $C_0(2)=-\frac{1}{4}$, and $C_0(3)=\frac{1}{16}$, with the additional convention that $C_l(j)=0$ for $j>2l+3$, and taking $C_l(-j)=-C_l(j)$. By using Eqs. (17), (19), and (20) we finally obtain

$$I(x_0)=\frac{n^2 2^{2l+3}}{\pi(l!)^2}\frac{(n-l-1)!}{(n+l)!} \times\sum_{j=1}^{2l+3} C(j)\left[\sum_{\alpha=2}^{2i_{\max}} s(\alpha)J(\alpha)+\sum_{\beta=1}^{i_{\max}} d(\beta)J(\beta)\right] \tag{22}$$

with

$$\left.\begin{matrix}J(\alpha)\\J(\beta)\end{matrix}\right\}=\frac{\sin^2[(\frac{1}{2}k+a)x_0]}{k+2a}+\frac{\sin^2[(\frac{1}{2}k-a)x_0]}{k-2a} , \tag{23}$$

where $a=N-\alpha$ for $J(\alpha)$ or $a=\beta-1$ for $J(\beta)$. Equation (22) allows a fast evaluation of $I(x_0)$ for all x_0 values [for $x_0\to 0$, i.e., for small K values, an expansion of Eq. (23) can be useful]. No numerical difficulties have been encountered even at the highest n values investigated ($n\sim 80$), owing to the symmetry property of the a_i coefficients and also to their explicit expression which shows that the terms of the summations over α and β are not spread out over too many order of magnitudes, thus avoiding numerical problems. This contrasts with the case where the Gegenbauer polynomials are expressed in terms of hypergeometric functions. Finally note that for most cases of practical interest we are interested in initial states of low angular momentum and therefore the summation over j contains few terms.

The case of s states ($l=0$) is somewhat apart, since all a_i coefficients are equal to unity and resummation of trigonometric lines is possible. In this case only it is better to start from the expression of the Gegenbauer polynomial (i.e., C^1_{n-1}) in terms of hypergeometric function [i.e., $C^1_{n-1}\sim F(1+n,1-n;\frac{3}{2};1/(n^2p^2+1))$]. The change of variable

$$\sin^2 y=\frac{1}{(n^2p^2+1)}$$

leads to

$$I(p_0)=\frac{8n}{\pi}\int_0^{y_0}\frac{\sin^3 y\sin^2(2ny)}{\cos y}dy \tag{24}$$

(s states), where $y_0=\arcsin(1/n^2p_0^2+1)$. After some lengthy and tedious algebra we obtain, for s states,

$$I(p_0)=I(y_0)=\frac{4n}{\pi}\left[-\frac{\sin^2 y_0}{2}+\frac{\sin^2(2ny_0)}{2n}+\frac{1}{4}\frac{\sin^2[(2n+1)y_0]}{(2n+1)}-\frac{1}{4}\frac{\sin^2[(2n-1)y_0]}{(2n-1)}-2\sum_{k=1}^{2n}(-1)^k\frac{\sin^2(ky_0)}{k}\right] . \tag{25}$$

For $y_0\to 0$ (i.e., for small K values) this expression reduces to

$$I(p_0)\to\frac{16n^3y_0^6}{3\pi}(1-n^2y_0^2+\tfrac{32}{75}n^4y_0^4\cdots) \text{ as } y_0\to 0 . \tag{26}$$

Equation (25) [or Eq. (26) if $ny_0\lesssim 0.3$] provides a very fast BET form-factor evaluation for s states. For other initial states (with $l\neq 0$) the BET form factor is computed from Eq. (22).

IV. CALCULATIONS OF THE CROSS SECTIONS FOR VARIOUS TYPES OF INTERACTION

First of all our main intention is to discuss the possible use of the BET form factor to compute cross sections according to Eq. (1). We have carried out extensive comparisons between BET and quantal cross sections in more than four hundred cases corresponding to various situations of practical interest. Before presenting some typical examples in detail (see Sec. V) we shall briefly review the cases investigated as well as the corresponding explicit expressions of Eq. (1).

For Rydberg-atom–atom collisions the (e^--$\mathscr{P}$) interaction is short range[24] (Fermi-type potential), the corresponding squared (e^--$\mathscr{P}$) scattering amplitude $|f_e(K)|^2$ being L^2 with L the scattering length. This, in fact, corresponds to a first-order expansion of the scattering amplitude.[25] Inclusion of further terms is possible,[4] within the scope of the scattering length approximation, but leads to complications unnecessary for our purpose. The scattering length being independent of K the integral in Eq. (1) reduces to:

$$\sigma_{if}=C\int_{K_{\min}}^{K_{\max}} F_{ij}(K)K\,dK \tag{27}$$

with $C=(2\pi L^2)/v^2$, where $K_{\min}=|k_i-k_f|$ and $K_{\max}=k_i+k_f$, the initial k_i and final k_f momentum being given by energy conservation factors:

$$k_i^2+2\mu E_i=k_f^2+2\mu E_f \tag{28}$$

with μ the reduced mass of the two colliding atoms. As mentioned in the introduction the only final states to be taken into account are the closest hydrogenic levels. For

example, Na(nd) states (quantum defect $\delta \simeq 10^{-2}$) will be mainly depopulated towards the $nf,ng,nh,\ldots$ levels. Similarly, Rb(ns) states (quantum defect $\delta \simeq 3.1$) will lead mainly to the $(n-3)f,(n-3),g,(n-3)h,\ldots$ exit channels. This process will be referred to as l mixing, though strictly speaking a change in the n value can also occur. Accordingly this quasielastic process induced by short-range interaction always involve small $|n-n'|$ values.

In the case of Rydberg-atom—molecule collisions the short-range (e^--molecule) interaction is still present and can be treated in a similar way, L being deduced from the low-energy elastic (e^--molecule) scattering data. This interaction leads also to the quasielastic l-mixing process, with no internal change in the rotational state of the molecular target. However, we also have to consider the long-range (e^--molecule) interaction which can be expressed as a multipolar expansion. The (e^--dipole) and (e^--quadrupole) interactions only are considered here. In this case rotational excitation (or deexcitation) of the molecule and subsequent deexcitation (or excitation) of the Rydberg atom occur, with possibly noticeable $|n-n'|$ values. The process can be very efficient, especially if the total energy in the entrance channel closely matches (within about 2 cm^{-1}) that in the exit channel.[26,17] As usual the squared scattering amplitudes are deduced from the first Born approximation. Their explicit expressions are given by

$$|f_e(J\to J'=J\pm 1;K)|^2=\frac{4}{3}\frac{J_M}{(2J+1)}\frac{D^2}{K^2} \tag{29}$$

for the dipolar case[27,28] [D being the dipole moment and $J_M=\max(J,J')$] and by

$$|f_e(J\to J'=J\pm 2;K)|^2=\frac{2}{15}\frac{J_M(J_M-1)}{(J+J_M)^2-1}Q^2 \tag{30}$$

for the quadrupolar case[29] (Q being the quadrupole moment). In the former case the integral in Eq. (1) reduces to

$$\sigma_{if}=C'\int_{K_{\min}}^{K_{\max}} F_{ij}(K)\frac{dK}{K} \tag{31}$$

with

$$C'=\frac{8\pi}{3v^2}\frac{J_M}{(2J+1)}D^2 ,$$

where $K_{\min}$ and $K_{\max}$ are given by Eq. (28), E_i and E_f being the total internal energy (including rotational energy) of the entrance and exit channels, respectively. The latter case (quadrupole interaction), the corresponding scattering amplitude being independent of K, is similar to that of the short-range interaction; thus, this case reduces to the computation of the integral given by Eq. (27) with

$$C=\frac{4\pi}{15v^2}\frac{J_M(J_M-1)}{(J+J_M)^2-1}Q^2 .$$

Finally, comparison between Eqs. (27) and (31) clearly shows that the dipolar case should be more sensitive than the other two cases to the accuracy of the calculated $F_{ij}(K)$ value for K close to $K_{\min}$, because of the $1/K$ factor.

The procedure used to obtain the cross-sections values discussed in the following section will now be dealt with in more detail. Firstly, the numerical integration of Eq. (27) [or (31)] has been performed for both BET and quantal calculations, through an adaptive Newton-Coates routine. Such a sophisticated routine, though necessary for the quantal calculations, is probably not needed for the BET calculations (see below). Secondly, for the sake of simplicity and analyticity [see Eq. (22)], hydrogenic wave functions are used. In practice, because the Rydberg state in the entrance channel is usually a nonhydrogenic state (n_0,l) of effective quantum number $n_0^*=n_0-\delta$, where δ is its quantum defect, we shall use for our calculations the quantum number n which is the closest integer to n_0^* together with the true energy of the level considered, (n_0,l).[30] For example, $n=29$ will be used for the calculations involving the Rb(32s) state, its quantum defect being about 3.1. Thirdly, it is worth mentioning that the BET calculations do not properly include transitions to nonhydrogenic states since all n' exit channels are assumed to have the same energy. This should not matter since in the case of Rydberg states the final nonhydrogenic levels of low multiplicity have already been shown to have a negligible contribution to the depopulation process.

V. COMPARISON BETWEEN BET AND QUANTAL CALCULATIONS

To our knowledge no calculations using the BET form factor are available for transitions with small $|n-n'|$ values. It is generally assumed that the BET method is not valid in such a case[17] (which covers in fact most existing experimental results). In our opinion this is by no means obvious in view of the derivation of the BET form factor (see Sec. II). Thus, we rely on a detailed comparison between BET and quantal calculations to answer the question convincingly, which is why most of the following examples deal with cases corresponding to small $|n-n'|$ values. Another reason for checking this controversial situation is that we recently performed measurements of the quenching cross sections of Rb(ns and nd) atoms colliding with CO molecule. This target having a small rotational B constant (~ 1.9 cm^{-1}) it is easy to show that the main inelastic channels leading to the quenching process are those with small ($\lesssim 10$) $|n-n'|$ values, owing to the relative population of the CO rotational levels in our cell experiment[26] (only those rotational levels with $J\lesssim 15$ are noticeably populated).

We now discuss in detail some typical examples. First the l-mixing process induced by the short-range (e^--$\mathscr{P}$) interaction is analyzed, the corresponding cross section being computed according to Eq. (27). The two examples chosen deal with one molecular (CO) and one atomic (He) target. Then the rotationally inelastic processes due to the long-range (e^--dipole) interaction are discussed in the case of Rb*-CO collisions, the corresponding cross sections being derived from Eq. (31). All the other cases checked display the same general features.

A. *l*-mixing process induced by the short-range interaction

1. Rb-CO*

It should first be noted that in this case $|n-n'|=0$. Let us take the following example:

$$\mathrm{Rb}(23d)+\mathrm{CO}\rightarrow\mathrm{Rb}(22f,22g,22h,\ldots)+\mathrm{CO}+\Delta E\ . \quad (32)$$

The Rb ($23d$) level has a quantum defect of about 1.35 and thus lies energetically close ($|\Delta E|\sim 0.4\ \mathrm{cm}^{-1}$) to the neighboring hydrogenic ($22f,22g,22h,\ldots$) levels. We consider only the short-range interaction between the outer electron and the CO molecule, leading to no rotational energy change of the CO target. Cross-section calculations are performed for $T=293$ K. The integration interval [Eq. (1)] ranges from about 0.13 to about 31. The quantal cross section is deduced from the sum of the partial cross sections ($23d\rightarrow 22l'$, $l'=3,\ldots,21$) computed according to Eq. (1) within the frame of the impulse approach. Thus, for each partial calculation the corresponding form factor $F_{23d\rightarrow 22l'}(K)$ has to be computed first, before the final integration is performed. BET results are obtained by first computing only the $F_{23d\rightarrow 22}(K)$ form factor according to Eqs. (14) and (22) and then integrating over K. Figures 1, 2, and 3 display various aspects of the calculations. Several comments can be made. First the

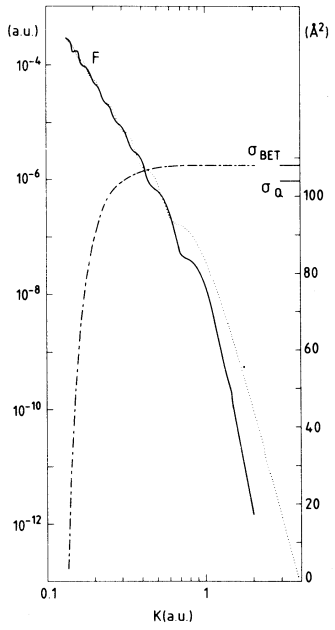

FIG. 1. Quantal (solid curve) and BET (dotted curve) form factor F for the ($23d\rightarrow 22$) transition in rubidium as a function of the momentum transfer K. Both quantities are expressed in atomic units. The left-hand scale refers to the form factor. The BET cross section for the process $\mathrm{Rb}(23d)+\mathrm{CO}\rightarrow\mathrm{Rb}(22f,22g,22h,\ldots)+\mathrm{CO}$, computed according to Eq. (27) is also reported (dot-dashed curve) as a function of the upper limit of integration [Eq. (27)]. The right-hand scale refers to the cross section (in $\mathrm{Å}^2$). Also shown are the quantal (σ_Q) and BET (σ_{BET}) cross-section values obtained for the true upper limit of integration $K_{\max}\simeq 31$.

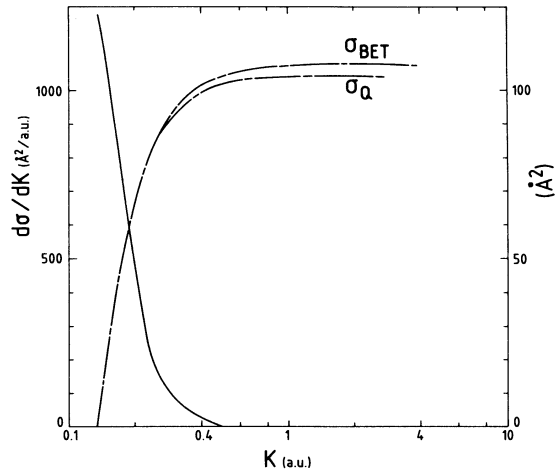

FIG. 2. BET (σ_{BET}) and quantal (σ_Q) cross sections for the process $\mathrm{Rb}(23d)+\mathrm{CO}\rightarrow\mathrm{Rb}(22f,22g,22h,\ldots)+\mathrm{CO}$ as a function of the upper limit of integration [Eq. (27)]. The right-hand scale refers to the cross sections (in $\mathrm{Å}^2$). The solid curve is the K derivative of the cross sections (BET and quantal calculations are almost undistinguishable). Values are in $\mathrm{Å}^2$ per atomic unit and correspond to the left-hand scale. The curve shows that K values between 0.5 a.u. and the upper limit of integration ($K_{\max}\simeq 31$ a.u.) contribute negligibly to the cross section.

BET and quantal form factors [the latter obtained by summing the partial form factors according to Eq. (3)] are in good agreement for K values less than about 0.6, though local differences can be observed (see Fig. 1). For higher K values the BET approximation appears unreliable, a point discussed qualitatively in Sec. II. Secondly, the cross sections deduced by the two methods agree within 4%, since only K values close to the lower limit of integration ($K<0.4$) contribute significantly to the cross

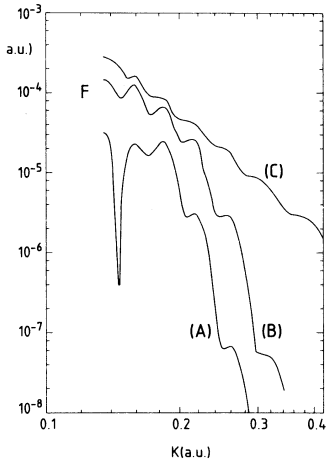

FIG. 3. Quantal form factors F (in atomic units) for some transitions in rubidium, as a function of the momentum transfer K (in atomic units). Curve (A) refers to the ($23d\rightarrow 22l'$, $l'=13$) transition. Curve (B) represents the sum over l' from 12 to 15 of the type (A) partial quantal form factors and curve (C) the sum for l' ranging from 3 to 21, which corresponds to the form factor given in Fig. 1 (see text for comments).

sections as shown by Fig. 2. Thirdly, the almost regular shape of the form factor (Fig. 1) explains why the integration over K is easy when the BET method is used. Figure 3 shows how the shape of the $F_{23d\to 22}(K)$ form factor arises from the sum of partial $F_{23d\to 22l'}(K)$ form factors that can exhibit very sharp variations over a small K interval: in spite of local accidents arising for various l' values, the shape of the summed curve is almost regular. This explains why sophisticated integration methods are required when computing partial cross sections by the quantal approach (see also the next example). Let us finally mention that a detailed comparison between BET and quantal calculations was carried out on Rb (ns and nd) states over a wide range of n values ($22<n<35$) for the titled process [Eq. (32)]. In all cases the cross sections obtained by the two methods agree to within less than 20%.

2. Na^*-He

Let us consider as a second example the l-mixing process induced by rare-gas atoms, a process widely investigated both experimentally[1] and theoretically[1,3,4,12] in the recent past. More specifically we shall deal with the following reaction:

$$\mathrm{Na}(nd)+\mathrm{He}\to\mathrm{Na}(nf,ng,nh,\ldots)+\mathrm{He}+\Delta E\ . \qquad (33)$$

The process is quasielastic since the Na(nd) states have a quantum defect of about 1.5×10^{-2}. BET and quantal calculations performed (at $T=420$ K) for n values ranging from 6 to 25 exhibit general features quite similar to those obtained from our first example. Figure 4 shows that the cross sections obtained by the two methods agree to within about 20% over the whole range of n values, the BET values lying systematically above the quantal results. Figure 5 shows in more detail the case of the 24d level (for which $|\Delta E|\sim0.24$ cm^{-1}), the corresponding integration interval ranging from $K_{\min}\sim1.5\times10^{-3}$ to $K_{\max}\sim9.3$. It is clear from Fig. 5 that for both calculations only K values less than about 0.1 contribute noticeably to the final result, i.e., the integral is sharply peaked

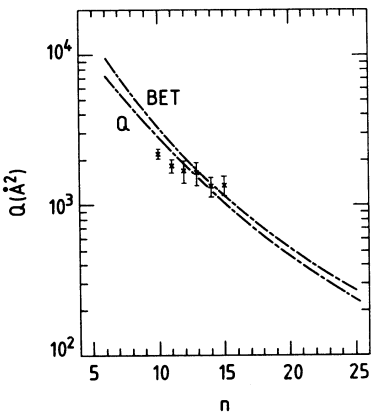

FIG. 4. Quantal and BET cross sections for the l-mixing process of Na nd states colliding with helium [Eq. (33)]. Also reported are the experimental results of Ref. 31.

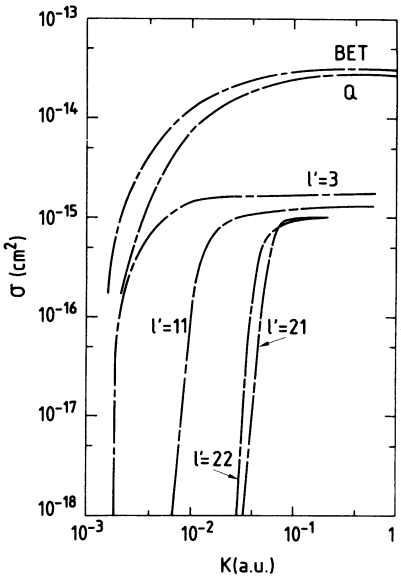

FIG. 5. The two upper curves represent the BET and quantal cross sections for the Na($24d$)+He→Na($24l'$, $l'=3,4,\ldots$) +He process as a function of the upper limit of integration [Eq. (27)]. The momentum transfer K is given in atomic units. The true limit of integration is $K\simeq9.3$ a.u., but both cross sections reach their final values of $K\sim0.1$ a.u. Also shown are some quantal partial cross sections, the corresponding l' value being indicated. All cross sections are in cm^{-2}.

in the vicinity of the $K_{\min}$ value, a fact already observed in the preceding example. It should be noted, however, that agreement between the two methods is not close, as in the first case (Fig. 2) for K values near the threshold $K_{\min}$ because, as shown later on, the BET approach appears less reliable when K is very small. This hardly affects the final cross section, however, since the final integration of Eq. (27) [i.e., $\int KF(K)dK$] gives little weight to $F(K)$ for the smallest K values ($K<10^{-2}$). Figure 5 also shows in addition that the K values corresponding to 90% of the cross sections can vary noticeably for different l' values. Finally, the efficiency of the BET approach can be judged from the fact that the BET calculation of the total cross section requires about 400 evaluations of the form factor while about 14 000 are necessary in the quantum case (in both cases a precision of 10^{-5} was requested), mainly owing to local accidents of the partial quantal form factors (Fig. 3). Moreover, the number of evaluations is almost independent of n for the BET method but increases drastically with n in the quantum case. This indicates that the BET form factor has a smooth K variation whatever the n value, a fact observed in all cases investigated.

B. Rotationally inelastic collisions induced by the long-range interaction

We now consider the collision induced by the long-range (Rydberg electron-dipole) interaction. The corresponding cross sections are computed according to Eqs. (1), (29), and (31). More specifically, let us take as our first example the process

$$\mathrm{Rb}(23d)+\mathrm{CO}(J=7)\rightarrow \mathrm{Rb}(23f,23g,23h,\ldots)+\mathrm{CO}(J=6)+\Delta E\ . \quad (34)$$

The reaction is quasiresonant since $\Delta E\sim 0.3\ \mathrm{cm}^{-1}$. The corresponding $K_{\min}$ and $K_{\max}$ values are 6.10^{-3} and 19.1, respectively. Calculations are performed at $T=293$ K, the CO dipole moment being taken as 4.4×10^{-2}. The results are given in Fig. 6. The BET cross section ($\sigma=8740$ Å^2) agrees well with the quantal result ($\sigma=8490$ Å^2). Only a small part of the K interval contributes to the cross section ($6.10^{-3}<K\lesssim 3.10^{-2}$) and in this range the two form factors are similar in shape, though noticeable local differences ($\sim 40\%$) can be observed. (Better agreement between the two form factor calculations is observed for $K\gtrsim 0.1$; for K values above about 0.6 the BET approach, as already noted, becomes unreliable). Tables I and II give a whole set of results obtained for both excitation and deexcitation of a CO molecule in collision with a Rb($23d$) atom (only e^--dipole interaction is taken into account). Comparison between BET and quantal cross sections shows very good overall agreement, the $|n-n'|$ values ranging from 0 to 6. Only when very high cross sections are obtained does the agreement seem to be possibly worse (within 50%). More precisely this situation can arise when the energy balance ΔE of the process is small ($<0.5\ \mathrm{cm}^{-1}$), i.e., when the threshold $K_{\min}$ value is less than about 10^{-2}. Such a situation is reported in Fig. 7 and corresponds to the process

$$\mathrm{Rb}(23d)+\mathrm{CO}(J=2)\rightarrow \mathrm{Rb}(22f,22g,22h,\ldots)+\mathrm{CO}(J=1)+0.4\ \mathrm{cm}^{-1}\ . \quad (35)$$

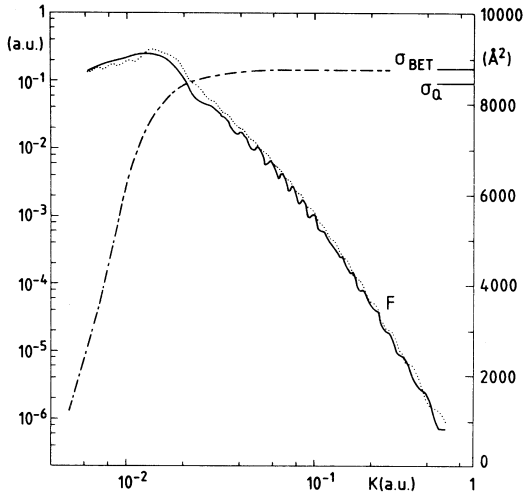

FIG. 6. Quantal (solid curve) and BET (dotted curve) form factor F for the $23d\rightarrow 23$ transition in rubidium as a function of the momentum transfer K. Both quantities are expressed in atomic units. The left-hand scale refers to the form factor. The BET cross section for the process $\mathrm{Rb}(23d)+\mathrm{CO}(J+7)\rightarrow \mathrm{Rb}(23f,23g,23h,\ldots)+\mathrm{CO}(J=6)$, computed according to Eq. (31) is also reported as a function of the upper limit of integration [Eq. (31)]. The right-hand scale refers to the cross section (in Å^2). Also shown on the scale are the BET and quantal (σ_Q) cross sections obtained for the true upper limit of integration $K_{\max}\simeq 19$ a.u.

TABLE I. BET (σ_B) and quantal (σ_Q) cross-section values (in Å^2) for the rotational deexcitation of CO molecule in collisions with Rb($23d$) atoms. Reported are the initial J value (the final value J' being $J-1$), the final Rydberg hydrogenic states n' and the energy defect ΔE (in cm^{-1}) for the process. Only processes with small ΔE values are considered since in other cases the cross sections are found to be negligible (see Ref. 26).

J	n'	ΔE	σ_Q	σ_B
1	22	−3.45	33.4	33.9
2	22	0.40	6220	9630
6	23	−3.51	40.2	41.1
7	23	0.33	8490	8740
11	24	−1.24	1040	1170
12	24	2.59	110	117
15	25	−0.85	2710	2670
16	25	2.98	66.8	69.6
18	26	−2.62	97.8	102
19	26	1.20	1440	1520
21	27	−2.97	58.7	61.6
22	27	0.84	1890	1840

Figure 7 shows that there is a systematic difference between the BET and quantal form factors (in contrast to Fig. 6) for K values below 4.10^{-2} a.u., leading to the observed difference between the quantal ($\sigma_Q=6220$ Å^2) and BET ($\sigma_{\mathrm{BET}}=9630$ Å^2) cross sections. From our last two examples it is clear that the behavior of the BET form factor for small K values ($K\lesssim 10^{-2}$) deserves further attention. It is important to note that, by contrast with the case of short-range or quadrupolar interaction the $F(K)/K$ form of the integrand magnifies the differences observed for $F(K)$ close to the threshold $K_{\min}$ value, in the cross section calculation for the e^--dipole interaction. Finally, numerous other levels are investigated and lead to similar conclusions: Only for transitions with very small $K_{\min}$ values can the BET and quantal cross sections be noticeably different. For all other cases remarkable agreement between the two calculations is observed.

We do not report here the case of (e^--quadrupole) interaction since, as already mentioned, it is quite similar to the short-range one. Very good agreement is found between BET and quantal cross-sections, as long as the K range considered lies typically between 5.10^{-3} and 1, which is the case for most situations of practical interest.

TABLE II. BET (σ_B) and quantal (σ_Q) cross-section values (in Å^2) for the rotational excitations ($J'=J+1$) of the CO molecule in collisions with Rb($23d$) atoms. For notations and comments see Table I.

J	n'	ΔE	σ_Q	σ_B
2	21	3.28	77.4	78.5
3	21	−0.56	4980	3950
9	20	1.89	324	334
10	20	−1.94	304	310
17	19	0.89	948	1160
18	19	−2.93	102	103

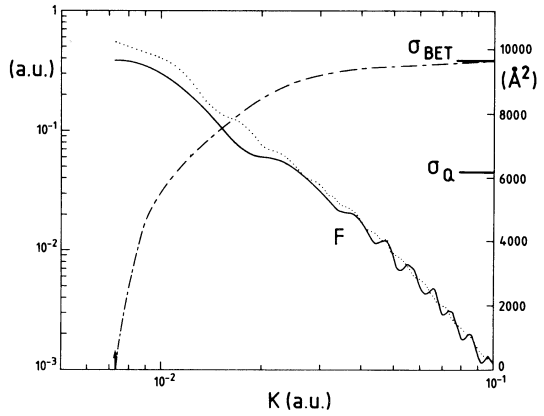

FIG. 7. Quantal (solid curve) and BET (dotted curve) form factor F for the $23d \rightarrow 22$ transition in rubidium as a function of the momentum transfer K. Both quantities are in atomic units. The left-hand scale refers to the form factor. Note that this corresponds to the case of Fig. 1, except that K values are smaller. The BET cross section for the process $Rb(23d)+CO(J=2) \rightarrow Rb(22f,22g,22h,\ldots)+CO(J=1)$, is also reported. Notations are those of Fig. 6. The K_{max} value for this case is about 19 a.u., the threshold value K_{min} being indicated by an arrow.

Here we shall not discuss the general features of the Rydberg-atom–dipolar-molecule collisions (i.e., the ΔE, n, and J variations of the corresponding cross sections): this problem is dealt with in another paper[26] devoted to an experimental study of Rb(ns and nd)-CO collisions, where detailed comparisons between experimental data and BET calculations are presented (they show a very good overall agreement). Finally the case of collisions involving large $|n-n'|$ values is also disregarded for two reasons: Firstly, our calculations concern only the CO molecule, which has a small rotational constant. In this case it is easy to show that such collisions contribute negligibly to the total depopulation of Rydberg states. Secondly, calculations using the BET approximation have already appeared in the literature[17] and the use of the BET method for such cases appears fairly noncontroversial.

VI. CONCLUSION

We have shown that the BET approximation provides a very efficient means of calculating the $(n,l \rightarrow n')$ cross sections corresponding to collisions between Rydberg atoms and atomic or molecular targets. This holds whatever the $|n-n'|$ value for various types of interaction, as demonstrated by a detailed comparison between BET and quantal calculations (for comparison between experimental and theoretical data we refer the reader to Ref. 26). We also give detailed information on the explicit expression of the BET form factor as well as on the corresponding numerical procedures. The tremendous gain in computation time offered by the BET method as compared with the quantal approach gives the former great advantage over the latter for the computation of collisional processes involving Rydberg states, especially because it seems to cover almost all situations of practical interest (except, perhaps, some sharply resonant processes). Finally the loss of information on partial $n,l \rightarrow n'l'$ transitions, a basic feature of the BET approach, is not a serious handicap in practice since most experiments only provide global information on the final exit channels.

ACKNOWLEDGMENTS

The authors would like to thank E. de Prunelé and B. Sayer for helpful discussions.

[1]An extensive review can be found in *Rydberg States of Atoms and Molecules,* edited by R. F. Stebbings and F. B. Dunning, (Cambridge University, Cambridge, New York, 1983).
[2]G. F. Chew and M. L. Goldberger, Phys. Rev. **87**, 778 (1952).
[3]A. P. Hickman, Phys. Rev. A **19**, 994 (1979).
[4]M. Matsuzawa, J. Phys. B **12**, 3743 (1979).
[5]Y. Hahn, J. Phys. B **14**, 985 (1981).
[6]E. de Prunelé, Phys. Rev. A **27**, 1831 (1983).
[7]M. R. Flannery, Phys. Rev. A **22**, 2408 (1980). See also Chaps. 6, 7, and 11 of Ref. 1.
[8]I. C. Percival and D. Richards, Adv. At. Mol. Phys. **11**, 1 (1975).
[9]M. Inokuti, Rev. Mod. Phys. **43**, 297 (1971).
[10]M. Matsuzawa, Phys. Rev. A **9**, 241 (1974).
[11]L. Y. Cheng and H. van Regemorter, J. Phys. B **14**, 4025 (1981).
[12]K. Sasano, Y. Sato, and M. Matsuzawa, Phys. Rev. A **27**, 2421 (1983).
[13]M. Hugon, F. Gounand, P. R. Fournier, and J. Berlande, J. Phys. B **13**, 1585 (1980).
[14]F. G. Kellert, K. A. Smith, R. D. Rundel, F. B. Dunning, and R. F. Stebbings, J. Chem. Phys. **72**, 3179 (1980). See also Chaps. 8 and 9 of Ref. 1.
[15]M. R. Flannery, Ann. Phys. (NY) **61**, 465 (1970). See also Chap. 11 of Ref. 1.
[16]M. Matsuzawa, J. Electron Spectrosc. Relat. Phenom. **4**, 1 (1974).
[17]M. Matsuzawa, Phys. Rev. A **20**, 860 (1979).
[18]L. Vriens, in *Case Studies in Atomic Collision Physics I,* edited by E. W. Mc Daniel and M. R. C. Mc Dowell (North-Holland, Amsterdam, 1969), p. 337.
[19]B. R. A. Nijboer and A. Rahman, Physica (Utrecht) **32**, 415 (1966).
[20]P. Eisenberg and P. M. Platzman, Phys. Rev. A **2**, 415 (1970).
[21]B. Podolsky and L. Pauling, Phys. Rev. **34**, 109 (1929).
[22]I. S. Gradshteyn and I. W. Ryzhik, *Table of Integrals Series and Products* (Academic, New York, 1965).
[23]M. Abramowitz and I. A. Stegun, *Handbook of Mathematical Functions* (Dover, New York, 1965).
[24]A. Omont, J. Phys. (Paris) **38**, 1343 (1977) and references therein.
[25]T. F. O'Malley, Phys. Rev. **130**, 1020 (1963).
[26]L. Petitjean, E. Gounand, and P. R. Fournier, Phys. Rev. A **30**, 71 (1984).
[27]K. Takayanagi, J. Phys. Soc. Jpn. **21**, 507 (1966).
[28]Y. Itikawa and K. Takayanagi, J. Phys. Soc. Jpn. **26**, 1254 (1969).
[29]N. F. Lane, Rev. Mod. Phys. **52**, 29 (1980).

[30]In fact, the cross section for Rb($32s$) will be obtained from a linear interpolation between the results computed for $n=29$ and 28 (see Ref. 13). However, this is irrelevant here since we will always compare BET and quantal calculations involving in both cases hydrogenic wave functions pertaining to the same n value (29 in this particular case). Moreover, the interpolation procedure leads to a final result that is only a few percent different from that obtained with the integer value closest to n_0. Note that, due to the form of Eq. (1) this is equivalent to an interpolation made on $F_{if}(K)$ between the two integers values closest to n_0 followed by the final integration over K [Eq. (1)]. It is important to realize that, for both the BET and the quantal case, the interpolation only affects the index n of the wave function and not the lower bound p_0 [Eq. (14); BET case] or $K_{\min}$, $K_{\max}$ [Eq. (1) for both cases] that are always computed for the true energy E_i of the entrance channel, thus taking into account its nonhydrogenic behavior. Finally, note that it is difficult, due to the detailed form of the $g_{nl}(p)$ function, to obtain simple n and n' scaling formulas for $F_{nl,n'}(K)$, except perhaps for very low and large K values. But this would be of little interest since these K ranges do not contribute significantly to the cross-section values (moreover, the BET method is not valid for large K values). Thus, it appears difficult to obtain a simple interpolation procedure on $F_{nl,n'}(K)$, in the K range of interest, when calculating p_0 [see Eq. (15)] for integer n values (instead of using the true energy of the studied level).

[31]T. Gallagher, S. A. Edelstein, and R. M. Hill, Phys. Rev. A **15**, 1945 (1977).